TẠP CHÍ KHOA HỌC VÀ CÔNG NGHỆ ĐẠI HỌC DUY TÂN
DTU Journal of Science and Technology 04(65) (2024) 80-89
TRƯỜNG ĐẠI HỌC DUY TÂN
DUYTAN UNIVERSITY

Classification of asphalt pavement crack severity using gradient boosting machine and image processing techniques

Phân loại vết nứt mặt đường sử dụng mô hình học máy tăng cường và các kỹ thuật xử lý ảnh

Hoang Nhat Duc[a,c*], Tran Van Duc[b,c], Nguyen Quoc Lam[c], Pham Quang Nhat[c]
Hoàng Nhật Đức[a,c*], Trần Văn Đức[b,c], Nguyễn Quốc Lâm[c], Phạm Quang Nhật[c]

[a]*Institute of Research and Development, Duy Tan University, Da Nang, 550000, Vietnam*
[a]*Viện Nghiên cứu và Phát triển Công nghệ Cao, Trường Đại học Duy Tân, Đà Nẵng, Việt Nam*
[b]*International School, Duy Tan University, Da Nang, 550000, Vietnam*
[b]*Viện Đào tạo Quốc tế, Trường Đại học Duy Tân, Đà Nẵng, Việt Nam*
[c]*Faculty of Civil Engineering, School of Engineering Technology, Duy Tan University, Da Nang, 550000, Vietnam*
[c]*Khoa Xây dựng, Trường Công nghệ, Trường Đại học Duy Tân, Đà Nẵng, Việt Nam*

(Date of receiving article: 16/03/2024, date of completion of review: 03/04/2024, date of acceptance for posting: 10/04/2024)

Abstract

This study puts forward an innovative approach for not only detecting cracks but also recognizing their severity. Herein, the severity of a crack object is characterized by its width. Light Gradient Boosting Machine (LightGBM) has been employed to categorize pavement surface into five labels: non-crack, sealed crack, minor crack, moderate crack, and severe crack. The model construction of the LightGBM requires a set of feature extractors, including steerable filters, projection integrals, and image texture analyses. Experimental results show that the LightGBM-based method is capable of achieving outstanding classification performance with CAR > 0.98 and F1 score > 0.95 for all class labels.

Keywords: asphalt pavement; crack severity; image processing; machine learning.

Tóm tắt

Nghiên cứu của chúng tôi đề xuất một phương pháp mới để phát hiện các vết nứt trên mặt đường và phân loại chúng dựa trên mức độ nghiêm trọng. Phương pháp học máy tăng cường dựa trên độ dốc (LightGBM) được sử dụng để phân loại bề mặt mặt đường thành năm nhóm: không nứt, nứt đã được trám, nứt nhỏ, nứt vừa, và nứt rộng. Chúng tôi sử dụng các bộ lọc có thể điều chỉnh, tích phân chiếu, và phân tích kết cấu hình ảnh để trích xuất tính chất của mẫu ảnh. Kết quả tính toán cho thấy phương pháp dựa trên LightGBM có khả năng phân loại tốt với độ chính xác lớn hơn 98% và chỉ số F1 lớn hơn 0.95 cho tất cả các nhóm ảnh.

Từ khóa: đường nhựa; mức độ của vết nứt; xử lý ảnh; học máy.

[*]*Corresponding author:* Hoang Nhat Duc
Email: hoangnhatduc@duytan.edu.vn

1. Introduction

Asphalt pavements have a crucial role in economic development and they bring about significant societal benefits. Hence, road infrastructure is one of the most important components of public assets. Due to extensive use and inclement weather conditions, pavement surfaces are often subjected to deterioration with many forms of distress such as fatigue, raveling, pothole, rutting, etc. Cracks appearing on the surface of asphalt pavement are generally the earliest sign of pavement failure. They reduce the strength of the pavement areas and allow water infiltration. If left untreated, the cracked surface may spread rapidly and deteriorate into other forms of damage such as raveling or potholes.

Hence, cracks should be detected early and require proper maintenance activities such as sealing or patching [1]. In addition, when detecting and measuring cracks, the severity of a crack object is also highly useful. Herein, the severity of pavement cracks can be categorized according to their width [2]. The information on crack severity can be particularly helpful for the task of maintenance prioritization. The manual surveying process, involving assessing and measuring crack objects, is notoriously time-consuming and unproductive. Moreover, this approach also yields inconsistent outcomes due to the subjective judgments of pavement inspectors. Hence, there is a pressing need to develop automated and efficient approaches for detecting and categorizing pavement crack severity with acceptable cost and computing requirements. These approaches can be applicable to small and local-level road maintenance authorities with limited resources.

In recent years, due to the rapid advancements of image processing techniques and the availability of low-cost cameras, various computer vision-based methods have been proposed to assist in the surveying process of pavement health conditions. Image processing has been intensively used and combined with machine learning to construct intelligent and automated approaches for pavement crack detection. According to recent reviews by Cano-Ortiz et al. [3] and Kheradmandi, Mehranfar [4], an increasing trend in automated pavement distress recognition can be observed. In addition, the utilization of image processing and machine learning methods is one of the prominent research directions. Hence, there is a practical need to investigate other advanced computer vision-based methods for dealing with the task of interest. Moreover, it can be seen from the current literature that most of the works focus on crack detection; computer vision-based crack severity recognition has rarely been evaluated.

In the field of automated monitoring of pavement defects, it can be observed that support vector machine and neural networks are dominant methods. However, gradient boosting machine (GBM) has been gaining more attention of the research community in recent years. This method constructs a model in the form of an ensemble of weak learners (e.g. classification trees). GBM aims at optimizing a cost function used to quantify a classifier's performance by iteratively driving the function's parameters in the direction of a negative gradient. This gradient-based optimization has brought about the development of various powerful boosting algorithms. Nevertheless, compared to the conventional approaches such as support vector machine and neural networks, the application of GBM in the field of crack appearance and crack property classification is still limited.

Among the variants of GBM, Light Gradient Boosting Machine (LightGBM), described by Ke et al. [5], is an advanced boosting framework used for pattern recognition. Two novel techniques of gradient-based one side sampling

and exclusive feature bundling are employed to enhance the classification performance of a LightGBM-based model. These two notable techniques provide the LightGBM with considerable edges over other machine learning approaches [6,7]. Therefore, the current works aim at harnessing the advantage of LightGBM in classification of pavement crack severity.

2. Research method

2.1. Image processing-based feature computation

2.1.1. Steerable filter (SF) and projection integral (PI) for computing edge-based features

The edge-based features of the region are crucial for identifying crack objects in an image region. This study employs the SF [8,9], which is an orientation-selective convolution kernel, to reveal the edge-related characteristics. The SF is capable of performing edge detection and noise suppression concurrently. Given a full scene of a pavement surface, an image patch with a specific size (e.g. 64x64 pixels) is separated for analysis. Within this image patch, a 2-dimensional Gaussian with a variance σ of a pixel is given by [8]:

$$G(x,y,\sigma)=\frac{1}{2\pi\sigma^2}\exp[\frac{-(x^2+y^2)}{2\sigma^2}] \quad (1)$$

where (x, y) denotes a pixel's coordinates.

On the basis of the two steerable filters with β = 0° and β = 90°, the PI, which is a popular *method for face recognition, can be constructed to characterize the shape of an object appearing* on the pavement surface. This paper relies on the horizontal PI (HPI), vertical PI (VPI), and two diagonal PIs. Previous studies have demonstrated their effectiveness in crack detection and classification [10,11]. Generally, an integral projection is a one-dimensional pattern; it is obtained via the sum of a given set of pixels along a given direction. The HPI and VPI are obtained by summing the pixels within an image patch along the horizontal and vertical directions. Meanwhile, to compute, the diagonal PIs of +45° and -45°, the image patch is first rotated with the corresponding angle; subsequently, the VPI of the rotated image can be calculated. A demonstration of the edge detection process based on SF and PI methods is provided in Fig. 1.

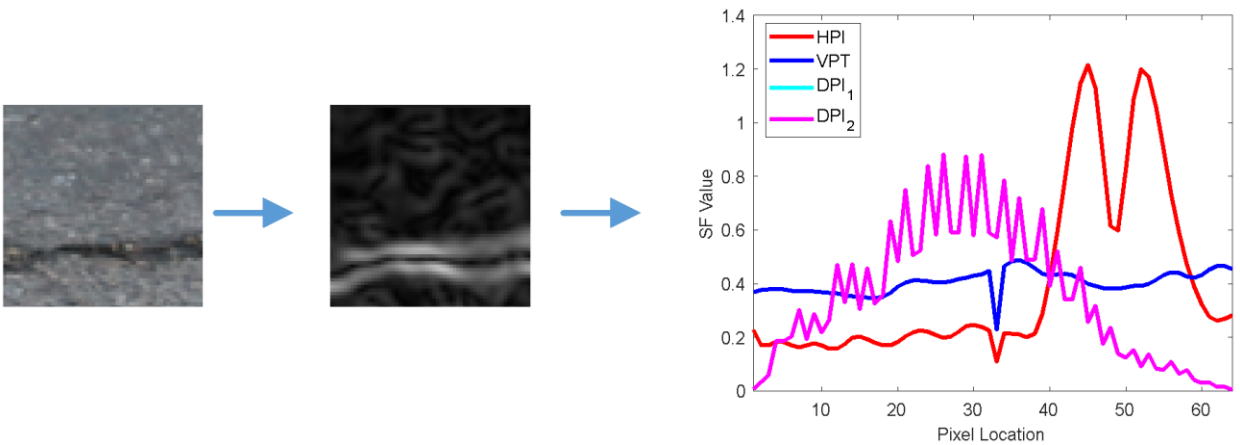

Fig. 1 Demonstration of the SF- and IP-based edge detection

2.1.2. Color-based texture descriptors

Due to the diversity of the pavement background, using the color-related features can help to distinguish crack objects from non-crack ones (e.g. dirt, traffic marks, etc.). Hence, this study utilizes the statistical properties of three color channels (red, green, and blue) of an image sample. Let I denote a matrix that stores the gray levels of an image sample and $P(I)$ represents the first-order histogram of I. Using $P(I)$, the

statistical measurements of a specific color channel can be computed [12]. These measurements include the mean, standard deviation, skewness, Kurtosis, entropy, and range of an image [13].

2.1.3. Local ternary pattern (LTP)

The LTP, proposed by Tan, Triggs [14], is an extension of the standard Local Binary Patterns (LBP) [15]. The LBP is an effective method for characterizing local structures of a gray-scale image. The local structure is calculated by comparing each pixel in the image with its eight neighboring pixels in the 3x3 neighborhood. The neighboring pixels are coded 1 if their gray intensity is greater than that of the center pixel and it is coded 0 otherwise. The capability of the LBP is greatly affected by illumination variations as well as random noise in near-uniform regions in images. To improve the standard LBP, Tan, Triggs [14] propose the LTP a variant of LBP. LTP employs a parameter to threshold pixels into three values to improve the discriminative power of the original LBP.

2.1.4. Centre symmetric quadruple pattern (CSQP)

The CSQP, put forward in [16], attempts to increase the neighborhood used in the conventional LBP. Instead of using a window size of 3x3, the CSQP employs a 4x4 neighborhood. It is because under complex variations in illumination and background, a large neighborhood may help reduce the intra-class dissimilarity. This texture descriptor aims to exploit the local relationships existing amongst the pixels via comparing the upper and the lower half of an image patch. In addition, the CSQP is designed to capture meaningful asymmetry in the diagonally opposite quadruple space within a 4x4 neighborhood.

2.1.5. Attractive repulsive center symmetric local binary pattern (ARCSLBP)

The ARCSLBP, proposed by El merabet et al. [17], compares the four center-symmetric pairs of pixels within a 3x3 neighborhood. Four triplets corresponding to the vertical, horizontal, diagonal directions can be established to describe a local structure of an image. In addition, local attractive-and-repulsive characteristics are considered so that the ARCSLBP is capable of capturing both gradient and textural information. The attractive and repulsive relationships between three pixels are determined by the attractive $\lambda_A(.)$, and repulsive $\lambda_R(.)$ binary thresholding functions. Generally, a triplet is formed by including three pixel values (g_i, g_c, g_j) where g_i and g_j are the gray intensities of the pair of opposite pixels and g_c denotes the gray intensity of the pixel at the center of a neighborhood. A triplet is attractive if the central pixel has a lower gray intensity than those of opposite neighboring pixels. Meanwhile, a triple is repulsive if the gray intensity of the central pixel is higher than those of opposite neighboring pixels [17].

2.2. Light gradient boosting machine (LightGBM)

The LightGBM, put forward by Ke et al. [5], is an effective implementation of the gradient boosting algorithm. This machine learning method extends the gradient boosting algorithm by utilizing a form of automatic feature selection and emphasizing on boosting data instances with larger gradients. These features help increase the computing efficiency and enhance the predictive performance of the LightGBM [18]. This machine learning method combines a set of weak decision trees to establish a robust ensemble. The training process of the LightGBM is performed progressively. Herein, a new LightGBM model is built by minimizing the classification error of the previous one.

The classification error is quantified by a loss function. For the task of classifying the pavement crack severity, the multi-class log loss can be used. The ensemble model $f(x)$ is

constructed by integrating a set of M individual trees as follows:

$$f(x) = \sum_{m=1}^{M} f_m(x) \quad (2)$$

where f_1, f_2,…,f_M are individual classification trees.

3. Experimental results and discussion

This section of the study is dedicated to reporting the performance of the newly developed computer vision-based method for categorizing the severity of pavement cracks. The proposed framework is a combination of LightGBM-based pattern recognition and image processing-based feature extraction. Notably, the data classification process of the LightGBM requires the image processing techniques of SF, PI, color channel analysis, and texture descriptors (LTP, CSQP, and ARCSLBP). It is worth noticing that the LightGBM model is constructed with the assistance of the Python library provided in [19]. The SF image processing technique is implemented with the MATLAB toolbox provided in [20]. The programs used to compute the color-based statistical indices, LTP, CSQP, and ARCSLBP have been coded in Visual C# .NET by the authors. The image thresholding method of Otsu and the morphological operators used to extract the objects of interest from the pavement image patches are carried out with the help of built-in functions in MATLAB's image processing toolbox [21].

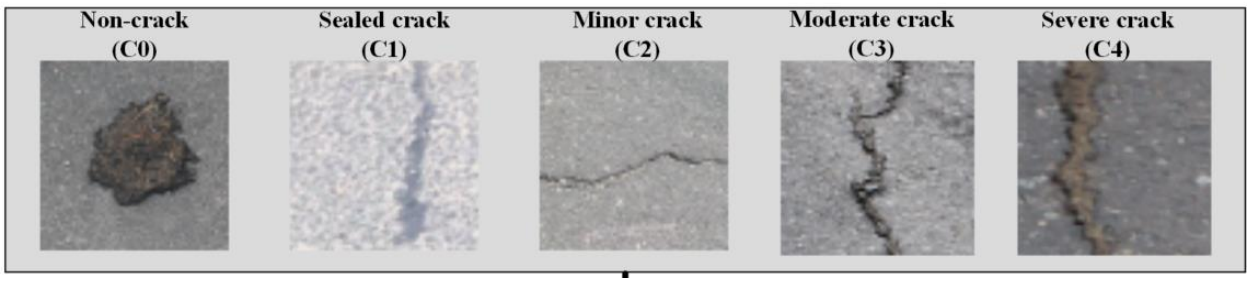

Fig. 2 The collected image dataset

An image dataset (refer to Fig. 2) containing five class labels is collected during field trips in Danang city (Vietnam). The class labels are non-crack (coded as C0), sealed crack (coded as C1), minor crack (coded as C2), moderate crack (coded as C3), and severe crack (coded as C4). Herein, the class C2 includes crack objects whose width is less than 1 mm. The width of cracks in the class C3 ranges from 1 mm to 3 mm. In addition, the class C4 contains the cracks whose width exceeds 3 mm. Each class label contains 625 instances to ensure a balanced classification of the data instances. The total number of the collected image samples is 3125. Hence, the data in each category accounts for 20% of the whole image dataset. The image samples are captured by the 18-megapixel resolution Canon EOS M10 at a distance of about 1.2m above the pavement surface. The data collection process aims to gather diverse image samples containing crack objects on various pavement backgrounds. In addition, data in the non-crack category includes commonly encountered objects such as traffic marks, blurred traffic marks, rutting, potholes, oil stains, bleeding, and raveling to ensure the generalization of the constructed computer vision-based model.

To ease the image processing phase, the sample size has been fixed to be 64x64 pixels. The ground truth labels of samples have been assigned by road inspectors. The collected image dataset is randomly separated into a training set (90%) and a testing set (10%). The

former is used for training the LightGBM model; the latter is used for evaluating the generalization of the machine learning models. As mentioned earlier, the SF coupled with PI is first used to analyze the edge-based features of the image. Consequently, the HPI, VPI, and two diagonal PIs are constructed. Each PI yields 64 sampling points. Hence, the total number of features computed by the PIs is 64x4 = 256. The approaches of median filter, Otsu method-based image thresholding, and morphological operations are used to extract the object of interest from the background. Herein, the employed morphological operations include connected component labeling and small object filtering. With each extracted object, the statistical measurements of color channels are computed. These statistical measurements are mean, standard deviation, skewness, Kurtosis, entropy, and range.

It is noted that the color-based features help to take into account the irregular objects such as traffic marks, stains, dirt, manholes, etc. existing on the pavement surface. Six features are computed for each color channel. Therefore, the number of color-based features is 6x3 = 18. In addition, to deal with the complexity of various crack patterns, this study relies on the state-of-the-art texture descriptors of the LTP, CSQP, and ARCSLBP. These descriptors are effective methods for capturing the local structure of pixels as well as handling lighting changes and rotation variations. These capabilities are highly useful for delineating crack patterns because crack objects in real-world circumstances are arbitrarily rotated and suffer from uncontrolled lighting conditions. The LTP, CSQP, and ARCSLBP are employed to calculate the texture-based features of each image block. The outputs of these texture descriptors are the histograms that represent the local structure, coarseness or fineness properties, and pixel distribution of an image sample. It is noted that the number of features extracted by the LTP, CSQP, and ARCSLBP is 116, 256, and 256, respectively.

It is noted that each component of the feature set plays a key role in characterizing the surface of asphalt pavement. In detail, the color-based feature helps delineate objects such as traffic marks and stains; the integral projections help recognize edge-based features in the image; and the local binary pattern-based approaches help describe textural features of the image. The combinations of the color-based features, the integral projections, and the local binary pattern-based features can be highly useful for recognizing defects in asphalt pavement [13].

Herein, a region of interest on a pavement is separated into blocks of equal size (e.g. 64x64 pixels). One pixel has an area of roughly 3.6 × 3.6 mm; thus, the actual pavement area in one image patch is approximately 230 × 230 mm. It is noted that the proposed method employs a block-based approach for detection and classification of cracks in large pavement images. An original image is first divided into non-overlapping blocks with the size of 64x64 pixels. Feature extraction phase is performed to calculate the textural characteristics of the image block. LightGBM analyzes the extracted features and yields the predicted class labels of the data sample.

As stated earlier, the PI-based and color-based extractors yield 256 + 18 = 274 features. This group of features is then combined with the LTP, CSQP, and ARCSLBP to form three sets of features:

(i) Feature set (FS) 1 includes the PI-based, color-based, and ARCSLBP features. The total number of features is 274 + 256 = 530.

(ii) Feature set (FS) 2 includes the PI-based, color-based, and CSQP features. The total number of features is 274 + 256 = 530.

(iii) Feature set (FS) 3 includes the PI-based, color-based, and LTP features. The total number of features is 274 + 116 = 390.

The datasets corresponding to these three feature sets can be accessed at https://github.com/NhatDucHoang/PaveCrackSeverityLightGBM. The input features used to categorize pavement crack severity have different ranges. Thus, to standardize the input ranges, the Z-score equation has been used. In addition, to assess the performance of the computer vision-based models, this paper employs the indices of classification accuracy rate (CAR), precision, recall, and F1 score.

The LightGBM is trained and tested with three datasets corresponding to three feature sets. It is noted that the experiments in this study were executed on the ASUS FX705GE - EW165T (Core i7 8750H and 8 GB Ram) platform. To fine-tune the hyper-parameters of the LightGBM model (the number of leaves, number of estimators, maximum depth, and learning rate), five-fold cross validation processes were performed. Using these cross validation processes, the dataset is divided into five mutually exclusive folds. In each run, one data fold serves as a testing dataset; the other data folds are used to train the machine learning model. The model's performance is assessed via the average F1 score obtained from the five testing data folds. Accordingly, the hyper-parameters of LightGBM with respect to three feature sets are given by:

(i) LightGBM using Feature Set 1: the number of leaves = 41, the number of estimators = 200, the maximum depth = 7, and the learning rate = 0.94.

(ii) LightGBM using Feature Set 2: the number of leaves = 41, the number of estimators = 200, the maximum depth = 9, and the learning rate = 0.85.

(iii) LightGBM using Feature Set 3: the number of leaves = 21, the number of estimators = 150, the maximum depth = 7, and the learning rate = 0.91.

Table 1. Result comparison

Class Labels	**Indices**	**LightGBM Feature Set 1**		**LightGBM Feature Set 2**		**LightGBM Feature Set 3**	
		Mean	Std	Mean	Std	Mean	Std
C0 (Non-crack)	CAR	0.9815	0.0077	0.9471	0.0149	0.9767	0.0118
	Precision	0.9447	0.0265	0.8500	0.0384	0.9493	0.0338
	Recall	0.9646	0.0207	0.8950	0.0494	0.9327	0.0373
	F1 Score	0.9543	0.0201	0.8711	0.0351	0.9405	0.0304
C1 (Sealed crack)	CAR	0.9976	0.0009	0.9982	0.0007	0.9975	0.0006
	Precision	0.9906	0.0030	0.9958	0.0023	0.9954	0.0029
	Recall	0.9974	0.0024	0.9952	0.0025	0.9920	0.0012
	F1 Score	0.9940	0.0022	0.9955	0.0017	0.9937	0.0016
C2 (Minor crack)	CAR	0.9802	0.0078	0.9514	0.0122	0.9714	0.0107
	Precision	0.9447	0.0251	0.8628	0.0346	0.9188	0.0425
	Recall	0.9557	0.0203	0.9081	0.0337	0.9386	0.0294
	F1 Score	0.9500	0.0195	0.8846	0.0298	0.9277	0.0238
C3 (Moderate crack)	CAR	0.9981	0.0006	0.9992	0.0004	0.9990	0.0006
	Precision	0.9975	0.0018	0.9973	0.0017	0.9959	0.0025
	Recall	0.9929	0.0032	0.9987	0.0011	0.9989	0.0013
	F1 Score	0.9952	0.0016	0.9980	0.0010	0.9974	0.0014

C4 (Severe crack)	CAR	0.9808	0.0074	0.9546	0.0120	0.9655	0.0102
	Precision	0.9499	0.0292	0.9039	0.0373	0.9196	0.0298
	Recall	0.9521	0.0331	0.8611	0.0372	0.9092	0.0360
	F1 Score	0.9504	0.0201	0.8815	0.0311	0.9138	0.0246

As stated earlier, the collected dataset, consisting of 3125 samples, is randomly divided into a training set (90%) and a testing set (10%). The first set is used for model training and the second set is used for model testing. Furthermore, to reduce the effect of random data sampling, this work has performed the model training and testing phases 20 times. In each run, 10% of the data samples are randomly selected to create a testing set. The statistical indices including mean and standard deviation (Std.) of the used measurement indices (CAR, precision, recall, and F1 score) are shown in Table 1.

It can be seen that the LightGBM with FS1 has achieved the highest performance in three out of five classes (C0: non-crack, C2: minor crack, and C4: severe crack). Meanwhile, the LightGBM with FS2 attains the best results in the C1 (sealed crack) and C3 (moderate crack). For the cases of C1 and C3, the performances of the three LightGBM models are very close to each other (their F1 scores > 0.99). However, when predicting data in C0, C2, and C4, the LightGBM with FS1 outperforms other models by a large margin.

It is also noted that the classification performance of all class labels is satisfactory. All CAR values surpass 98%. The data instances in C1 (sealed crack) and C3 (moderate crack) are classified with relatively higher CAR values. However, the discrepancy in classification performance among the five labels is only about 1%, which is relatively minor. Therefore, there are no significant differences in detection accuracy among different crack severity levels. In our opinion, this small degree of discrepancy in CAR among the classes can be attributed to certain randomness in the data sampling process.

Regarding the computational time, the LightGBM with FS1, FS2, and FS3 requires 2.53 s, 2.79 s, and 2.43 s, respectively. These are the average periods of time spent on training and testing the LightGBM model. Thus, it can be seen that the computational cost of the LightGBM using FS1 is slightly lower than that using FS2. Moreover, the classification performance of the model relying on FS1 is better than that employing FS2 by a large margin. These facts confirm the advantage of LightGBM in handling high-dimensional datasets.

4. Conclusion

This research aims at developing a novel computer vision-based approach for categorizing the severity of asphalt pavement cracks. The LightGBM integrated image processing techniques are used to classify samples of the pavement images into five labels: non-crack, sealed crack, minor crack, moderate crack, and severe crack. Moreover, image processing techniques, including the SF, PI, color-based features, and advanced texture descriptors, are employed to characterize the pavement surface condition. Herein, the LTP, CSQP, and ARCSLBP are used to represent the local structure of an image pixel and construct a set of features that are relevant for delineating different levels of crack severity.

A dataset, including 3125 image samples, has been collected to train and test the proposed computer vision-based method. Experimental results have confirmed the outstanding performance of the proposed LightGBM-based method. The feature set that includes the PI-based, color-based, and ARCSLBP-based

texture descriptors has demonstrated the best outcome with F1 scores greater than 0.95 for all class labels. The classification accuracy rates surpass 98% for all crack types. Hence, the newly developed computer vision approach can be a promising alternative to assist road maintenance authorities in the task of pavement survey.

Supplementary material

The dataset used to support the findings of this study has been deposited in the repository of GitHub at https://github.com/NhatDucHoang/PaveCrackSeverityLightGBM.

References

[1] Hoang N-D, Huynh T-C, Tran X-L, Tran V-D. (2022). A Novel Approach for Detection of Pavement Crack and Sealed Crack Using Image Processing and Salp Swarm Algorithm Optimized Machine Learning. *Advances in Civil Engineering* 2022:9193511. doi:10.1155/2022/9193511

[2] Liu F, Liu J, Wang L. (2022). Deep learning and infrared thermography for asphalt pavement crack severity classification. *Automation in Construction* 140:104383. doi:https://doi.org/10.1016/j.autcon.2022.104383

[3] Cano-Ortiz S, Pascual-Muñoz P, Castro-Fresno D. (2022). Machine learning algorithms for monitoring pavement performance. *Automation in Construction* 139:104309. doi:https://doi.org/10.1016/j.autcon.2022.104309

[4] Kheradmandi N, Mehranfar V. (2022). A critical review and comparative study on image segmentation-based techniques for pavement crack detection. *Construction and Building Materials* 321:126162. doi:https://doi.org/10.1016/j.conbuildmat.2021.126162

[5] Ke G, Meng Q, Finley T, Wang T, Chen W, Ma W, Ye Q, Liu T-Y (2017) LightGBM: a highly efficient gradient boosting decision tree. P*aper presented at the Proceedings of the 31st International Conference on Neural Information Processing Systems, Long Beach, California, USA*,

[6] Saber M, Boulmaiz T, Guermoui M, Abdrado KI, Kantoush SA, Sumi T, Boutaghane H, Nohara D, Mabrouk E. (2021). Examining LightGBM and CatBoost Models for Wadi Flash Flood Susceptibility Prediction. *Geocarto International*:1-27. doi:10.1080/10106049.2021.1974959

[7] Chun P-j, Izumi S, Yamane T. (2021). Automatic detection method of cracks from concrete surface imagery using two-step light gradient boosting machine. *Computer-Aided Civil and Infrastructure Engineering* 36 (1):61-72. doi:https://doi.org/10.1111/mice.12564

[8] Freeman WT, Adelson EH. (1991). The design and use of steerable filters. *IEEE Transactions on Pattern Analysis and Machine Intelligence* 13 (9):891-906. doi:10.1109/34.93808

[9] Perona P. (1995). Deformable kernels for early vision. *IEEE Transactions on Pattern Analysis and Machine Intelligence* 17 (5):488-499. doi:10.1109/34.391394

[10] Hoang N-D, Nguyen Q-L, Bui DT. (2018). Image Processing-Based Classification of Asphalt Pavement Cracks Using Support Vector Machine Optimized by Artificial Bee Colony. *Journal of Computing in Civil Engineering* 32 (5):04018037. doi:doi:10.1061/(ASCE)CP.1943-5487.0000781

[11] Cubero-Fernandez A, Rodriguez-Lozano FJ, Villatoro R, Olivares J, Palomares JM. (2017). Efficient pavement crack detection and classification. *EURASIP Journal on Image and Video Processing* 2017 (1):39. doi:10.1186/s13640-017-0187-0

[12] Theodoridis S, Koutroumbas K (2009) Pattern Recognition. *Academic Press*, Printed in the United States of America, ISBN 978-1-59749-272-0

[13] Hoang N-D. (2019). Automatic detection of asphalt pavement raveling using image texture based feature extraction and stochastic gradient descent logistic regression. *Automation in Construction* 105:102843. doi:https://doi.org/10.1016/j.autcon.2019.102843

[14] Tan X, Triggs B. (2010). Enhanced Local Texture Feature Sets for Face Recognition Under Difficult Lighting Conditions. *IEEE Transactions on Image Processing* 19 (6):1635-1650. doi:10.1109/TIP.2010.2042645

[15] Ojala T, Pietikainen M, Harwood D Performance evaluation of texture measures with classification based on Kullback discrimination of distributions. I*n: Proceedings of 12th International Conference on Pattern Recognition*, 1994-10 1994. pp 582-585 vol.581. doi:10.1109/ICPR.1994.576366

[16] Chakraborty S, Singh SK, Chakraborty P. (2018). Centre symmetric quadruple pattern: A novel descriptor for facial image recognition and retrieval. *Pattern Recognition Letters* 115:50-58. doi:https://doi.org/10.1016/j.patrec.2017.10.015

[17] El merabet Y, Ruichek Y, El idrissi A. (2019). Attractive-and-repulsive center-symmetric local binary patterns for texture classification. *Engineering Applications of Artificial Intelligence* 78:158-172. doi:https://doi.org/10.1016/j.engappai.2018.11.011

[18] Brownlee J. (2020). How to Develop a Light Gradient Boosted Machine (LightGBM) Ensemble. Machine Learning Mastery *<https://machinelearningmasterycom/light-gradient-boosted-machine-lightgbm-ensemble/>*

[19] Microsoft. (2022). LightGBM's documentation. *<https://lightgbmreadthedocsio/en/v332/> (Last access date: 7/14/2022)*

[20] Lanman D. (2006). Steerable Gaussian Filters. MATLAB Central *<https://wwwmathworkscom/ matlabcentral/fileexchange/9645-steerable-gaussian-filters>*

[21] MathWorks (2017) Image Processing Toolbox User's Guide. *MathWorks, Inc., https://www.mathworks.com/help/pdf_doc/images/images_tb.pdf (Last Access Date 06/12/2018), Natick, Massachusetts*.